ELSEVIER

Available online at www.sciencedirect.com

SCIENCE DIRECT®

Journal of Crystal Growth 281 (2005) 255–262

JOURNAL OF CRYSTAL GROWTH

www.elsevier.com/locate/jcrysgro

GSMBE growth and characterizations of AlInP/InGaAsP strain-compensated multiple-layer heterostructures

Z.C. Huang, H.Z. Wu*, Y.F. Lao, M. Cao, C. Liu

State Key Laboratory of Functional Materials for Informatics, Shanghai Institute of Microsystem and Information Technology, Graduate School of Chinese Academy of Sciences, Shanghai 200050, China

Received 28 January 2005; accepted 11 April 2005
Available online 13 June 2005
Communicated by M. Schieber

Abstract

We have grown long-period AlInP/InGaAsP strain-compensated multiple-layer heterostructures (SCMLHs) and SCMLHs combined with InAsP/InGaAsP strain-compensated multiple quantum wells (SC-MQWs) by gas source molecular beam epitaxy. Etch pit density (EPD) for both structures are in magnitude of $\sim 10^5\,cm^{-2}$. The increment of EPD with increase of period number is small, indicating low sensitivity of the dislocation density to the increase of period number of SCMLHs. High resolution X-ray diffraction and photoluminescence (PL) characterizations of the two structures demonstrate that crystal quality remains high due to strain compensation. Diffusion and segregation of indium were clearly observed in both InGaAsP and AlInP layers by secondary ion mass spectroscopy. As the thickness of epilayers increases In content increases, while Al decreases. PL for the structure of 20-pair AlInP/InGaAsP SCMLHs + InAsP/InGaAsP SC-MQWs shows strong luminescence and narrow line width. The strain-compensated technique can effectively suppress the formation of misfit dislocations in AlInP/InGaAsP SCMLHs although the thicknesses of epilayers are above the critical thickness of consisting materials, which may render its potential application in optoelectronic devices.
© 2005 Elsevier B.V. All rights reserved.

PACS: 68.35.−p; 81.15.Hi; 61.72.−y

Keywords: A1. Dislocations; A1. Strain compensated; A3. Gas source molecular beam epitaxy

1. Introduction

Long-wavelength (1.3–1.55 μm) vertical-cavity surface-emitting lasers (LW-VCSELs) are promising for application in optoelectronic devices. Compared with edge-emitting lasers, VCSELs

*Corresponding author. Tel.: +86 021 62511070; fax: +86 021 62513510.
E-mail address: hzwu@mail.sim.ac.cn (H.Z. Wu).

0022-0248/$ - see front matter © 2005 Elsevier B.V. All rights reserved.
doi:10.1016/j.jcrysgro.2005.04.062

exhibit advantages, such as low threshold current, single mode operation, high coupling efficiencies into fibers, and high-speed modulation. Up to date short wavelength VCSELs, such as 850 and 980 nm VCSELs have been commercialized [1]. However, it is still a challenge to realize LW-VCSELs because of the absence of high refractive index contrast semiconductor material system for distributed Bragg reflectors (DBRs) that are lattice matched to InP substrate [2]. In order to figure out this problem, various technologies have been tried, such as wafer bonding of GaAs-grown DBRs onto InP-grown active layers, dielectric mirrors, InP/air-gap DBRs, etc. [3,4]. However, the bonding technology is not easily compatible with full-wafer processing and testing capabilities, which constitute the major advantages of the VCSEL geometry for industrial fabrication [4]. The dielectric mirrors cannot be electrically conductive and inhibit homogeneous current injection into the active region [5]. The drawback of InP/air-gap DBRs is a complicated fabrication process and of low thermal conductivity [6].

In this paper, we proposed and studied AlInP/InGaAsP strain-compensated multiple-layer heterostructures (SCMLHs) that can be directly grown on InP substrate. A potential application of SCMLHs is to construct strain-compensated distributed Bragg reflector (SC-DBR) by using long-period ($\lambda/4$) SCMLHs. Strain compensation growth technique that decreases net strain in heterostructures by alternatively growing compressive- and tensile-strain layers, has been successfully employed in the growth of multiple quantum wells (MQWs) [7–9]. In the AlInP/InGaAsP SCMLHs, InGaAsP layer has compressive strain, while AlInP layer has tensile strain. The refractive index of AlInP is smaller than of InP, while the refractive index of compressively strained InGaAsP can be higher than the lattice matched InGaAsP by adjusting the compositions of indium and gallium in the InGaAsP layer. Thus, these materials combination has a larger refractive index contrast than that of the conventional lattice-matched InP/InGaAsP or InAlAs/InGaAlAs material systems ($\Delta n < 0.2$). A concern of applying the AlInP/InGaAsP SCMLHs to the SC-DBR is the presumable formation of dislocations when the thicknesses of consisting layers are larger than their critical thickness due to the lattice mismatch to InP substrate because dislocations will degrade the optical performances of DBR and even deteriorate active region of devices. It is expected that strain compensation should reduce the density of dislocations in the long-period AlInP/InGaAsP SCMLHs. In this work, we grew long-period ($\lambda/4$) AlInP/InGaAsP SCMLHsP by gas source molecular beam epitaxy (GSMBE). The microstructural and luminescent properties of the structures are characterized by etch pit density (EPD) observation, secondary ion mass spectroscopy (SIMS), X-ray diffraction (XRD), and photoluminescence (PL).

2. Experimental procedures

Strain-compensated AlInP/InGaAsP SCMLHs and InAsP/InGaAsP strain-compensated multiple quantum wells (SC-MQWs) were grown by Thermal V90 GSMBE system. The indium and gallium vaporized from thermal cell, and the aluminum vaporized from K-cell. As_2 and P_2 were obtained by cracking the AsH_3 and PH_3 gas when the gases flowed along a cracker, which was set at 1040 °C. The n-type dopant was silicon (Si) effused from a high-temperature effusion cell. The flux of group III elemental source was measured by an ion gauge to adjust the composition of In, Ga, Al in epitaxial layers. The flux of As_2 and P_2 are controlled and adjusted by the pressure of AsH_3 and PH_3.

Firstly, a 10-priod AlInP/InGaAsP SCMLHs doped with Si ($n_e = 2.5 \times 10^{18}\,cm^{-3}$) was grown at 510 °C. The growth rate was 3.0 and 3.0 Å/s for InGaAsP and AlInP, respectively. The thickness of AlInP layer and InGaAsP layer are 106.0 and 97.0 nm, respectively. The lattice mismatch ($\Delta a/a$) are 0.65% and −0.39% for compressively strained InGaAsP layer and for tensile-strained AlInP layer, respectively. In order to realize sharp interface and avoid the As_2 diffusion into AlInP layer, a schematic growth sequence at the interface of AlInP/InGaAsP SCMLHs is shown in Fig. 1. After the growth of 10-period SCMLHs and optimization of growth parameters, 20-pair

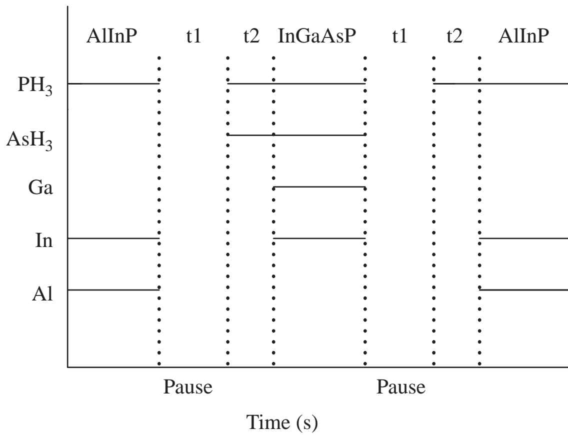

Fig. 1. Schematic illustration of growth sequence at the interface of AlInP/InGaAsP. The pause time (t_1) is 20 s. The interruption time (t_2) under PH_3, AsH_3 before InGaAsP layer growth and under AsH_3 before AlInP layer growth is 5 s.

AlInP/InGaAsP SCMLHs covered with 3-period InAsP/InGaAsP strain-compensated quantum wells was grown, which is schematically shown in Fig. 2. The structure started with a 250 nm thick n-type InP buffer layer, followed by 20-pair AlInP (106.0 nm) /InGaAsP(97.0 nm) layer, a 65.5 nm thick undoped InP spacer layer, 3-period undoped InGaAsP(10 nm)/InAsP (9.5 nm) strain-compensated quantum wells . Then the structure ends with a 65.5 nm thick undoped InP cap layer. The growth temperature is 510 °C for SCMLHs and 485 °C for SC-MQWs. All materials were grown on n-type InP(1 0 0) substrates with $n_e = 1{\sim}3 \times 10^{18}\,cm^{-3}$.

The etch pit observation is a convenient and effective method to obtain the density of the dislocations because there is a one-to-one correspondence between the etch pit and dislocations [10]. The Huber etchant ($2H_3PO_4$:1HBr) was used to produce the etch pit on the surface of different structures [11]. Firstly, the wafers were cleaned by isopropanol, acetone, and ethanol sequentially in ultrasonic bath, rinsed by deionized (DI) water, and dried with N_2. Then the wafers were etched for 3 min in $2H_3PO_4$:1HBr solution at 20 °C. A Normaski optical microscope was used to observe the etch pits. The dislocation density was characterized by EPD. The vertical composition

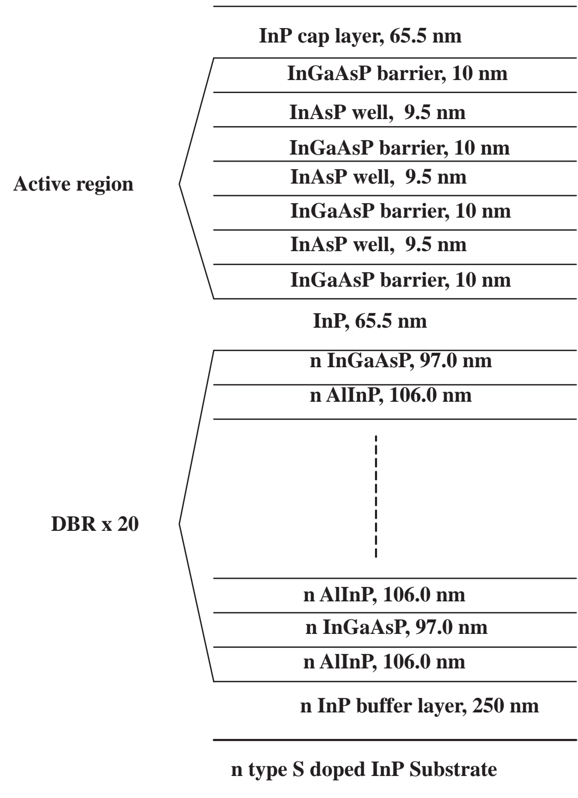

Fig. 2. Schematic illustration of AlInP/InGaAsP SCMLHs structure covered with InAsP/InGaAsP SC-MQWs.

diffusion was characterized by SIMS. A Philips MRD high-resolution X-ray diffractometer (HRXRD) employing Cu-K_α radiation monochromatized by a Ge (2 2 0) monochromator was used to record rocking curves of the (0 0 4) reflections and reciprocal space map close to (0 0 4) interface using triple-axis mode. Room temperature PL was carried out to characterize the SC-MQWs on the SCMLHs structure.

3. Results and discussions

The critical thickness for a strained epilayer was defined by Matthews' and Blakeslee's theory [12,13]. The critical thickness for InGaAsP layer with 0.66% mismatch to InP is 49 nm and for AlInP layer with −0.39% mismatch to InP is 89 nm. Actually, the experimentally measured

critical thickness is always larger than the calculated one by this model, which has been reported in several papers [14,15]. Although the thicknesses of the consisting layer of AlInP/InGaAsP SCMLHs are much larger than the critical thickness, it can be expected that the strain relaxation can be partly suppressed and the density of dislocation generated in the SCMLH can be low down by introduction of strain compensation. Accordingly, the strain-compensated technique was introduced to increase the number of periods in SCMLHs by alternative growth of InGaAsP and AlInP epilayers.

The etch pit patterns of InP substrate, InGaAsP single layer (1200 nm), 10-pair AlInP/InGaAsP SCMLHs (2030 nm), and 20-pair SCMLHs + SC-MQWs (4259.5 nm) are shown in Fig. 3. Fig. 3(a) is the etch pit pattern of InP substrate corresponding to EPD at the magnitude of $5.8 \times 10^4\,cm^{-2}$. Although the EPD of InGaAsP layer is about $1.34 \times 10^5\,cm^{-2}$, high-density parallel cracking lines are clearly seen in Fig. 3(b). This can be attributed to the full strain relaxation of InGaAsP layer, which is much larger than the critical thickness for InGaAsP/InP heterostructure. Fig. 3(c) and (d) show that the EPD of 10-pair AlInP/InGaAsP SCMLHs is $3.0 \times 10^5\,cm^{-2}$ and the EPD of 20-pair AlInP/InGaAsP SCMLHs + InAsP/InGaAsP SC-MQWs is $3.7 \times 10^5\,cm^{-2}$. By comparing Fig. 3(b) and (c), it is seen that although the EPD in the 10-pair SCMLHs is higher than that observed in single InGaAsP layer, the parallel cracking lines that are obviously observed in single InGaAsP layer are not present in the SCMLHs any more, indicating higher crystal quality of the 10-pair SCMLHs. This observation is in consistent with the following HRXRD measurement. Although the total thickness of 20-pair SCMLHs is double of the 10-pair SCMLHs, EPD number almost keeps constant.

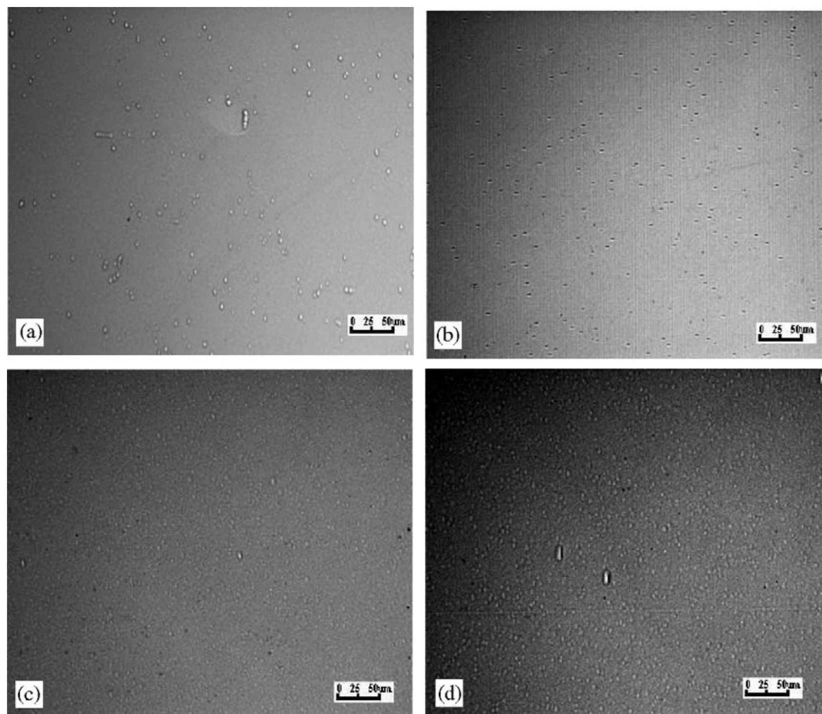

Fig. 3. Etch pit patterns. (a) Etch pits on etched surface of InP substrate. (b) Etch pits on etched surface of InGaAsP (1200 nm) single layer. (c) Etch pit on etched surface of 10-pair AlInP/InGaAsP SCMLHs. The top layer is InGaAsP layer. (d) Etch pit on etched surface 20-pair AlInP/InGaAsP SCMLHs surface covered with SC-MQWs.

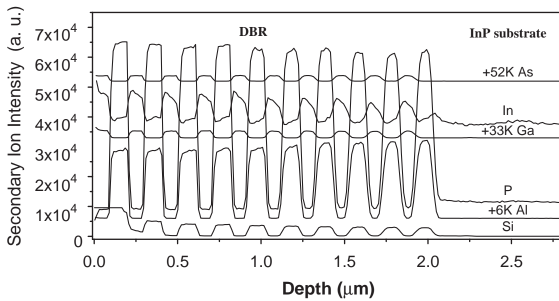

Fig. 4. SIMS result of AlInP/InGaAsP SCMLHs structure grown on an InP substrate. Silicon is the dopant of the material system.

Fig. 4 shows the secondary ion mass spectroscopy (SIMS) result of 10-pair AlInP/InGaAsP SCMLHs. Diffusion and segregation of indium were clearly observed in both InGaAsP and AlInP layers. The content of indium in SCMLHs gradually increased with the increase of epilayer thickness. On the contrary, the content of aluminum decreased with the increase of epilayer thickness. The different diffusion behavior of In and Al agrees well with Mozume's results [16]. Meanwhile, due to the longer duration at high growth temperature of 510 °C composition interdiffusion in bottom region is greater than that in the top region of the SCMLHs. Correspondingly, the interfaces close to surface is sharper than the interfaces close to substrate. From the SIMS results it is seen that the lower growth temperature is beneficial to the suppression of indium diffusion and segregation.

Fig. 5 shows the (0 0 4) diffraction rocking curves of the two SCMLHs. In Fig. 5(a), the envelope at the left of substrate peak is the diffraction of InGaAsP layer, and the right envelope displays diffraction of AlInP layer. The presence of a large number of satellite peaks proves the high crystalline quality of the 10-pair SCMLHs. The measured curve (i) and simulated curve (ii) are in good agreement, which is consistent with the observation of the relatively low dislocation density in the 10-pair metamorphic AlInP/InGaAsP SCMLHs. By comparison with the simulated curve, the satellite peaks of experimental curve are broadened and the peak intensity is lowered. These arise from the imperfections in

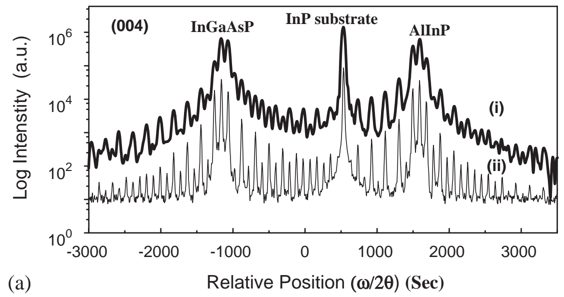

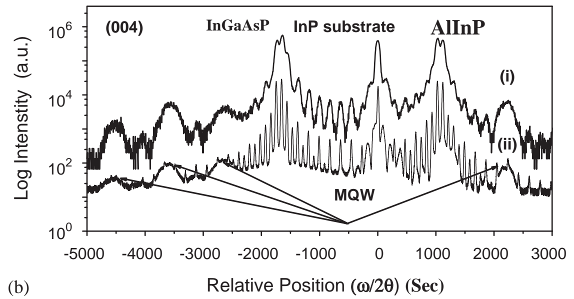

Fig. 5. (a) HRXRD rocking curves for 10-pair AlInP/InGaAsP SCMLHs: (i) measurement, (ii) simulation; (b) HRXRD rocking curves for 20-pair AlInP/InGaAsP SCMLHs + InAsP/InGaAsP SC-MQWs: (i) measurement, (ii) simulation.

SCMLHs, such as period fluctuation, composition diffusion that is observed in SIMS results, and the formation of misfit dislocations (MD) due to partly relaxation of strain [17]. From Fig. 5(a), it is difficult to separate the contribution of the rocking curve broadening from period fluctuation, MD, and element diffusion. To find out which component is main factor to the imperfection in the SCMLHs, period fluctuation, and MD were characterized using reciprocal space mapping which will be discussed later. Fig. 5(b) shows the (0 0 4) diffraction rocking curve of 20-pair AlInP/InGaAsP SCMLHs + InAsP/InGaAsP SC-MQWs. The main peak positions of experimental curve and simulated one are in very good agreement. But the satellite peaks are a little broadening and peak numbers were decreased by comparison with 10-pair SCMLHs. These may arise from period fluctuations, composition diffusion, and interface roughness by contrast to 10-pair SCMLHs [18]. So the crystal quality lowered and more misfit dislocations generated with the increase of period number. However, similar to the

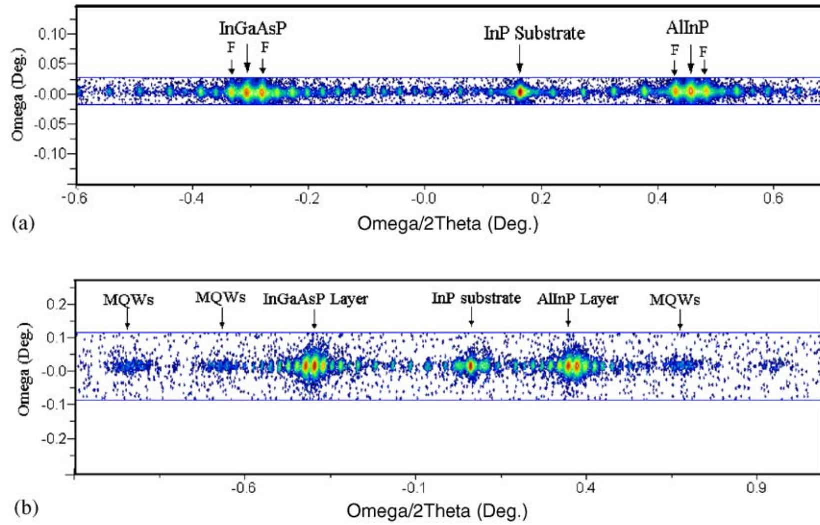

Fig. 6. Reciprocal space maps (004) of 10-pair AlInP/InGaAsP SCMLHs (a) and 20-pair AlInP/InGaAsP SCMLHs + InAsP/InGaAsP SC-MQWs (b) in which the reciprocal lattice points spread wider along $\Omega/2\theta$ than Ω-direction, indicating that the MD of 20-pair SC- SCMLHs is higher than that of 10-pair SCMLHs.

result of EPD method, HRXRD demonstrates the crystal quality does not degrade significantly.

Fig. 6 shows the reciprocal space maps (RSPs) of the 10-pair SCMLHs and the 20-pair AlInP/InGaAsP SCMLHs + InAsP/InGaAsP SC-MQWs. In Fig. 6(a) the diffuse scattering can be seen clearly. It is attributed to the existence of dislocation and rough interface resulted from In diffusion at the AlInP/InGaAsP heterointerface [18–20]. The reciprocal space points have a little broadening along ω-axis, and the average full-width at half-maximum (FWHM) of RSPs is 31 s in ω-direction. It is due to the presence of MD in the SCMLHs and the dislocations network leading to mosaic blocks. Accordingly, different orientations of mosaic blocks caused the broadening along ω-direction, which is also called mosaic spread. Along $\omega/2\theta$-direction the average FWHM of RSPs is very small ($\sim$16 s), indicating negligible deviation of SCMLHs period from the designed values. These results indicate that the peak broadening in Fig. 5 is due to the formation of MD, but not the period deviations of SCMLHs.

It can be seen that the RSPs quality of the structure shown in Fig. 6(b) slightly degrades compared with 10-pair SCMLHs in Fig. 6(a). The RSPs are slightly distorted, the number decreased, and the intensity of MQWs peaks is weak. An average FWHM (68 s) of RSP along ω-direction is related to the relatively higher dislocation density and larger mosaic spread by contrast with 10-pair SCMLHs. Again, the average FWHM (22.5 s) along $\omega/2\theta$-direction is larger than that of 10-pair SCMLHs as well. It can be expected that the period fluctuation increases with the number increase of epilayer pairs. However, from the result of average FWHM (22.5 s) along $\omega/2\theta$-direction, it can be concluded that the period fluctuation is not significant and the effect of period fluctuation on peak broadening along $\omega/2\theta$ in Fig. 5 is negligible by comparison to the effect of interface component diffusion and MD.

Although strain-compensated technique has been employed, the densities of MD are in the order of $\sim 10^5\,\mathrm{cm}^{-2}$. Moreover, the degree of relaxation will be enhanced with the increase of epilayer periods. According to the reported studies, the tensile-strain epilayers have lower quality than compressive strain epilayers. Tensile-strained films tend more to form faceted growth, surface composition modulations, and rough interface by comparison to compressive strain films [21,22]. For the strain-compensated AlInP/InGaAsP

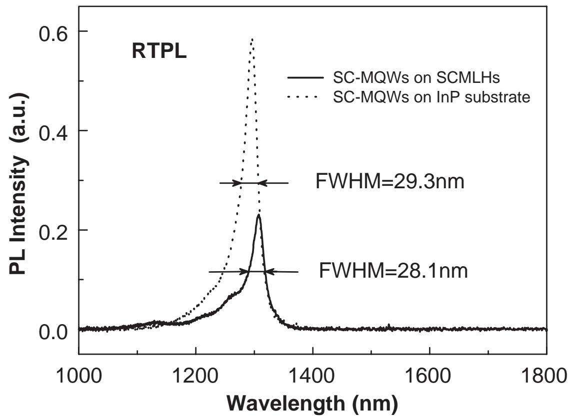

Fig. 7. RTPL spectra of 3-period InAsP/InGaAsP SC-MQWs on 20-pair AlInP/InGaAsP SCMLHs and 3-period SC-MQWs directly grown on InP substrate.

SCMLHs the most important impact on its quality is the dislocation density and interface roughness.

To evaluate the influence of strain relaxation on luminescence, room temperature photoluminescence (RTPL) measurement for SCMLHs + $3\times$ InAsP/InGaAsP SC-MQWs has been carried out. Fig. 7 shows the RTPL for structures of 20-pair AlInP/InGaAsP SCMLHs + $3\times$ InAsP/InGaAsP SC-MQWs and $3\times$ InAsP/InGaAsP SC-MQWs which was directly grown on InP substrate. The peak positions of the two structures are at 1297 and 1309 nm, respectively. The PL intensity of the former structure is third of the latter. However, the FWHM of PL peak of InAsP/InGaAsP SC-MQWs deposited on 20-pair AlInP/InGaAsP SCMLHs is 28.1 nm. It is 1.2 nm narrower than the directly grown $3\times$ InAsP/InGaAsP SC-MQWs which has the FWHM of 29.3 nm. Comparing with Lei's experiments [23], the narrow peaks prove the good quality of both samples. However, the lower PL intensity and narrower FWHM measured from the sample of 20-pair AlInP/InGaAsP SCMLHs + $3\times$ InAsP/InGaAsP SC-MQWs seems tergiversating. This phenomenon can be explained by optical cavity filtering effect on the measured PL. The 20-pair AlInP/InGaAsP SCMLHs forms bottom cavity mirror and the surface of InP cap layer forms top mirror (with reflectivity of ~27%). The modulation of PL by the optical cavity can be seen from the appearance of shoulder at about 1260 nm. Therefore, the observed PL intensity is lowered by the cavity filtering effect. It can be concluded that the thread dislocations generated from SCMLHs and penetrating into SC-MQWs is lower, otherwise the PL intensity of SC-MQWs grown on the 20-pair AlInP/InGaAsP SCMLHs will deteriorate significantly.

4. Summary

In summary, we have grown 10-period AlInP/InGaAsP SCMLHs and 20-pair AlInP/InGaAsP SCMLHs + InAsP/InGaAsP SC-MQWs by GSMBE method using growth interrupt technique. EPD for both structures are of magnitude $\sim 10^5\,\mathrm{cm}^{-2}$. The increment of EPD with the increase of period number is small. Thus, the dislocation density is not sensitive to the increase of period number of SCMLHs. Both HRXRD and PL characterizations of the structures demonstrate that crystal quality keeps high due to strain compensation. Diffusion and segregation of indium were observed in both InGaAsP and AlInP layers by the SIMS. The different diffusion behavior of In and Al are also observed. RTPL for the structure of 20-pair AlInP/InGaAsP SCMLHs + InAsP/InGaAsP SC-MQWs still demonstrates strong luminescence and narrow line width. The strain-compensated growth technique can effectively suppress the formation of MD and cracking lines in AlInP/InGaAsP SCMLHs although the thicknesses of epilayers are above each critical thickness, which may render its potential application in optoelectronic devices.

Acknowledgement

This work is supported by the National Key Basic Research Special Foundation of China under Grant No. 2003CB314903.

References

[1] S. Robert, M. Ortsiefer, J. Rosskopf, G. Böhm, C. Lauer, M. Maute, M. Amann, Proc. SPIE 5364 (2004) 1.
[2] M. Ortsiefer, R. Shau, G. Böhm, F. Köhler, M.C. Amann, Appl. Phys. Lett. 76 (2000) 2179.

[3] D. Babic, K. Streubel, R. Mirin, N. Margalit, J. Bowers, E. Hu, IEEE Photon Technol. Lett. 7 (1995) 1225.
[4] C.J. Chang-Hasnain, IEEE Opt. Commun. (2003) S30.
[5] G. Almuneau, E. Hall, S. Nakagawa, J.K. Kim, D. Lofgreen, O. Sjölund, C. Luo, D.R. Clarke, J.H. English, L.A. Coldren, J. Vac. Sci.Technol. B 18 (2000) 1601.
[6] S. Rapp, Long-Wavelength Vertical-Cavity Lasers Based on InP/GaInAsP Bragg Reflectors, Royal Institute of Technology, Stockholm, 1999, p. 23.
[7] B. Miller, U. Koren, M.G. Young, M.D. Chien, Appl. Phys. Lett. 58 (1991) 1952.
[8] H.Y. Chung, G. Stareev, J. Joos, M. Golling, J. Mähnß, K. Ebeling, J. Crystal Growth 201–202 (1999) 909.
[9] Y.G. Zhang, J.X. Chen, Y.Q. Chen, M. Qi, A.Z. Li, K. Fröjdh, B. Stoltz, J. Crystal Growth 227–228 (2001) 329.
[10] K. Akita, T. Kusunoki, S. Komiya, T. Kotani, J. Crystal Growth 46 (1979) 783.
[11] A. Huber, N.T. Linh, J. Crystal Growth 29 (1974) 80.
[12] J.W. Matthews, A.E. Blakeslee, J. Crystal Growth 27 (1993) 118.
[13] A. Braun, K.M. Briggs, P. Böni, J. Crystal Growth 241 (2002) 231.
[14] R. Beanland, D.J. Dunstan, P.J. Goodhew, Adv. Phys. 45 (1996) 87.
[15] H. Sugiura, M. Ogasawara, M. Mitsuhara, H. Oohashi, T. Amano, J. Appl. Phys. 79 (1996) 1233.
[16] T. Mozume, N. Georgiev, H. Yoshida, J. Crystal Growth 227–228 (2001) 577.
[17] K. Matney, M.S. Goorsky, J. Crystal Growth 148 (1995) 327.
[18] P.F. Fewster, Semicond. Sci. Technol. 8 (1993) 1915.
[19] M.S. Goorsky, M. Meshkinpour, D.C. Streit, T.R. Block, J. Phys. D: Appl. Phys. 28 (1995) A92.
[20] P.F. Fewster, Appl. Surf. Sci. 50 (1991) 9.
[21] T. Okada, G.C. Weatherly, J. Crystal Growth 179 (1997) 339.
[22] X. Wallart, O. Schuler, D. Deresmes, F. Mollot, Appl. Phys. Lett. 76 (2000) 2081.
[23] H.P. Lei, H.Z. Wu, Y.F. Lao, M. Qi, A.Z. Li, W.Z. Shen, J. Crystal Growth 256 (2003) 96.